The 31st International Workshop on Water Waves and Floating Bodies, Ann Arbor, MI, USA 2016

Experimental and numerical study of waves amplified by a submerged plate

Jonathan B. Duffett[1*], Robert F. Beck[1], Xiao Zhang[1], Kevin J. Maki[1], J.N. Newman[2]

[1]Department of Naval Architecture and Marine Engineering University of Michigan
Ann Arbor, MI, 48109 USA, *corresponding author e-mail: jduffett@umich.edu
[2]e-mail: jnn@mit.edu

Introduction

In the last workshop in Bristol, Newman (2015) presented results from linear potential wave theory that predicts that waves could be strongly amplified when traveling over a specially designed horizontal flat plate. In this work we study a similar plate that has a hole in the center to minimize nonlinear shallow-water effects. Furthermore the design was chosen to avoid extremely shallow submergence, and it has finite thickness. In this paper, we present results from physical experiments and viscous flow calculations together with the linear potential theory to further examine the wave amplification phenomenon. In general the agreement between the experiment, computational fluid dynamics (CFD), and linear theory is excellent. At the optimal wave number the linear theory slightly overpredicts the wave amplification.

Experimental Setup

The physical experiment is conducted at the University of Michigan Marine Hydrodynamics Laboratory in Ann Arbor, MI. This facility features a tow tank that has length 109.7 m, width 6.7 m, and average water depth of 3.2 m. The tank is equipped with a wedge-type wave maker at one end and a beach at the other. The diffraction plate is placed at a depth of 9.144 cm below the calm-water surface at mid-tank.

The diffraction plate is constructed of four sheets of 9.525 mm marine-grade plywood that are laminated together using thickened epoxy. The total thickness is approximately 20.63 mm. The shape of the plate was designed using the technique developed by Newman (2015) while keeping the plate within the constraints of the test facility. A schematic of the plate is shown in Figure 1. The plate has an inner radius of 0.5837 m and an outer radius R that is represented by the Fourier series (coefficients are in units of m):

$$R(\theta) = 1.101 + 0.02207\cos(2\theta) - 0.05983\cos(4\theta) + 0.05345\cos(6\theta) - 0.02186\cos(8\theta)$$

The edges of the plate are rounded with radius equal to half the thickness. The plate is sealed using epoxy and smoothed with 300 grit sandpaper. The plate is supported by four Unistrut stanchions and attached to the plate by 2.54 cm diameter threaded galvanized steel rods to allow for height adjustment. To ensure that the structure is sufficiently rigid it was statically load tested by hanging weights from the model and inspecting the deflection visually. The weights were sized using the force and moment predictions from WAMIT and including a safety factor. No noticeable deflection was observed. The natural frequency of the structure is much larger than the incident-wave frequency.

The free-surface elevation is measured with both sonic and capacitance wave probes. Eight Senix TSPC-30S1-232 ultrasonic sensors are used in the positions shown in Figure 1. Two capacitance

wave probes are also used at locations 3 and 5 in test cases where the free surface slope was too great for the ultrasonic sensors to function properly. Additionally, two dual-axis inclinometers are used near the upstream and downstream edges of the plate to measure plate rotation. All sensors are calibrated in accordance with manufacturer's instructions (data from the capacitance wave probes is post-processed further to adjust for frequency dependence).

The test matrix is chosen in order to examine both wave frequency and amplitude dependence. The wavelength varies between 1.98 m and 2.36 m. An analysis similar to Newman (2015) indicates that a wavelength of 2.18 m is optimal for wave amplification. The wave amplitude is varied from 3.175 mm to 15.875 mm in order to examine the influence of wave nonlinearity. The steepest in the experimental test plan had a height-to-amplitude ratio of 1:66, and most conditions had steepness in the range of 1:200. In order to limit the influence of the residual wave energy from a previous run, a subsequent run is not started until the maximum low-frequency free surface fluctuation decays to less than 0.5 mm. The results are presented using the dimensionless wave number $k^* = kc_0$ and steepness $s = 2a_0/\lambda$, where $c_0 = 1.101$ m is the length scale of the plate, a_0 is the amplitude of the incident wave, and $\lambda = 2\pi/k$ is the incident wavelength.

Experiments are conducted for 21 total wave conditions, and 17 sets of data are used for the analysis (4 were eliminated from the results based on sensor malfunction). The wave-amplification factor A^* is defined as the average wave amplitude at the origin (center of the plate) normalized by the average wave amplitude upstream that is measured by sensor 6: $A^* = \bar{a}_3/\bar{a}_6$. The average wave amplitude $\bar{a}_j$ is one-half of the average wave height in a time range of ten seconds. The wave height is measured from peak to trough.

CFD Simulations

The interaction of a regular wave with the submerged plate is also studied using a computational-fluid-dynamics approach. The interFoam solver from the open source CFD library OpenFOAM is used together with the open source waves2Foam library (Jacobsen (2011)). OpenFOAM uses the finite-volume method to solve partial differential equations on unstructured discretization of the domain. InterFoam solves the single-fluid conservation of mass and momentum equations for an incompressible fluid with spatially varying mechanical properties of density and molecular viscosity. The interface between the air and water phases is captured using the volume-of-fluid approach. A subset of seven cases are chosen to compare with the experimental measurements.

The computational domain extends from (x, y, z) = (-5.0, 0.0, -2.2) m to (5.0, 3.0, 0.5) m. Note that the lateral dimension of the computational domain is slightly less than the tank width. The depth of the computational domain is suitable for deep-water waves. The longest wavelength studied with the CFD solver has a length of 2.36 m.

The fluid grid is generated with the semi-automatic grid generator snappyHexMesh. The nominal cell size is 0.02 m. Stretching is used in the vertical direction such that the vertical spacing is 0.004 m near the free surface. Local refinement is to resolve the region around the plate such that the edge lengths in the region of the body are 0.0025 m. Boundary layer prisms are used to permit accurate wall-normal gradient calculation and the near wall spacing is 0.00035 m.

Results

The time series for the optimal condition, $k^* = 3.18$, $s = 0.00584$, is shown in figure 2. The vertical axis is the amplification factor. The horizontal lines correspond to the WAMIT prediction. The red line is the CFD, and the blue line is the experiment. The transient nature of the wave elevation in the center of the plate is clearly seen. Also, the CFD and the experiment show that the

trough elevation is larger than the peak elevation. In order to characterize the amplification factor a subset of the time history is used that starts after the wave system fully develops but before wave reflection becomes noticeable. In this case the time record from 30 to 40 seconds is used (shown in figure 3). In figure 3 the shape of the wave elevation shows that higher-frequencies are present in the solution. Note that the incident wave has a height-to-length ratio of 1:174. The wave height predicted by the CFD is significantly larger than that shown in the experimental measurement.

A second run is shown in figure 4 for $k^* = 2.93$ and $s = 0.00806$. In this case the higher harmonic is much more pronounced in the CFD and experiments. The incident wave-height-to-length ratio is 1:124. In this case the amplification factor is slightly larger for the CFD and experiments as compared to the WAMIT prediction.

The amplification factor for each experimental and CFD case is computed using the average of the wave heights in a time window of 10 s. The results are shown together with the WAMIT prediction in figures 5 and 6. The experimental measurements are shown with circular symbols, the CFD predictions are shown with square symbols, and the WAMIT predictions are shown with a blue line. The vertical line shows the optimal wave number. In this figure it can be seen that the experimental and CFD test plans focused on the optimal wave number and wave that are slightly longer and shorter. At the lowest wave number, the CFD predictions show a slightly lower amplification factor than that predicted by linear theory, whereas the experiments are consistently high of CFD and linear theory. At the optimal wave number, the linear theory predicts the highest amplification factor of 4.8. The CFD predicts between 4.1 and 4.5. The experiments showed a cluster of data which range from 3 to 4.1. It is not surprising that the linear theory predicts amplification that is greater than what is seen in the experiments and the CFD because without damping one would expect a resonance phenomenon to be overpredicted. The highest wave number indicates correlation between the CFD and WAMIT results that is similar to the low wave number cases. The experiments in this regime are in good agreement with the two numerical strategies.

In figure 6 the amplification factor is shown as a function of the steepness, and the symbols are colored with wave number. In this figure is appears that incident wave steepness does not play an identifiable role in the amplification of the wave. This is true for all wave numbers tested. For the largest experimental steepness that was tested ($s = 0.015$ or $2a/\lambda \approx 1/66$) wave breaking was observed in the region near the center of the plate. If the wave is amplified by a factor of 3 the steepness of the local wave becomes 1/22 and closer to a breaking regime.

Acknowledgment: The authors would like to thank the staff at the University of Michigan Marine Hydrodynamics laboratory for their assistance in conducting the experiments. The construction of the experimental apparatus was financially supported by the Couch Professorship. The authors are grateful for the support of the Office of Naval Research through the grants N00014-13-1-0558 and N00014-14-1-0577, administered by Kelly Cooper.

References

Newman, J.N. 'Amplification of waves by submerged plates,' 30th IWWWFB, Bristol, UK (2015).

OpenFOAM. The Open Source CFD Toolbox, Ver. 2.4.x (2015).

Jacobsen, N.G., and Fuhrman, D.R., and Fredsoe, J., 'A wave generation toolbox for the open-source CFD library: OpenFOAM,' *Int. J. Numer. Meth. Fluids* (2011).

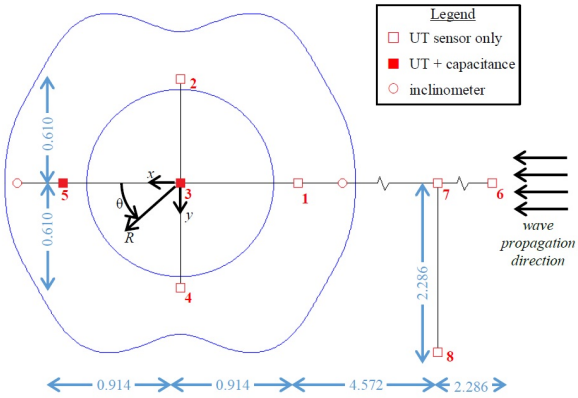

Fig. 1: Geometry of diffraction plate and test setup, distances are in m

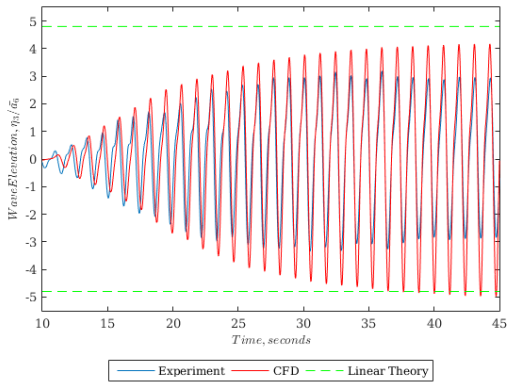

Fig. 2: Wave elevation for $k^* = 3.18$, $s = 0.00584$

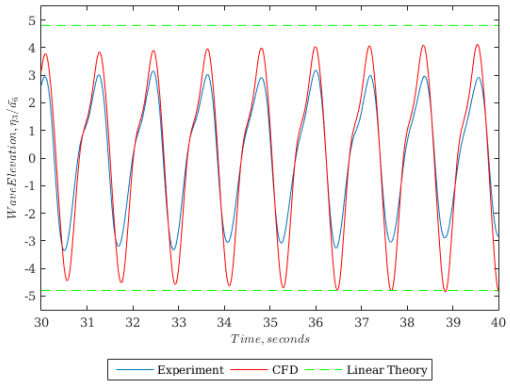

Fig. 3: Wave elevation for $k^* = 3.18$, $s = 0.00584$

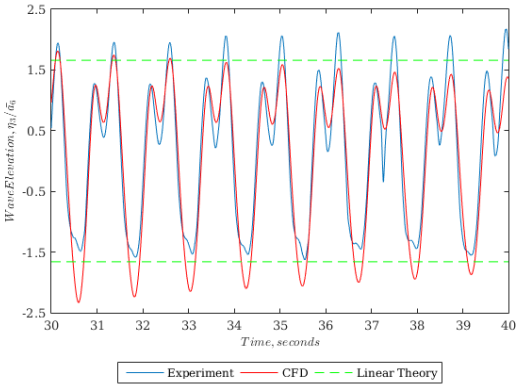

Fig. 4: Wave elevation for $k^* = 2.93$, $s = 0.00806$

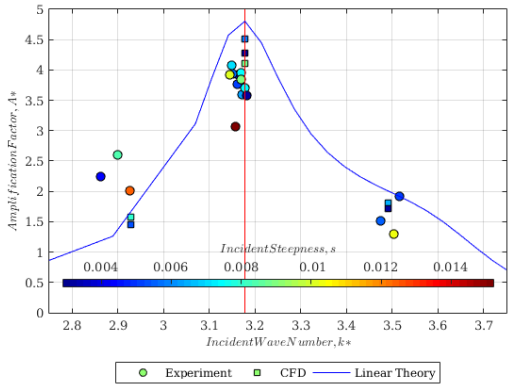

Fig. 5: Amplification factor on wave number

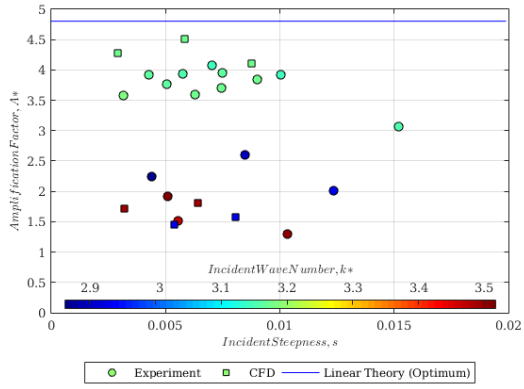

Fig. 6: Amplification factor on wave steepness